Magazine of Civil Engineering

ISSN 2712-8172

journal homepage: http://engstroy.spbstu.ru/

Research article

UDC 691.335

DOI: 10.34910/MCE.116.11

Processing, characterization and hardening mechanism of one-part geopolymer cement

H.M. Khater, A.M. El Nagar, M. Ezzat✉

Housing and Building National Research Center, Cairo, Egypt
✉ *topaz75@gmail.com*

Keywords: mechanical properties, smart materials, multifunctional composites, engineering properties, microstructure imaging

Abstract. Sustainable development of technologies for the industrial waste utilization for building construction areas are given considerable worldwide attention due to their advantages in reduction of greenhouse gases compared to Portland cement as well as conservation of raw materials resources used in cement production. Therefore, geopolymer materials are introduced, not only for the environmental issue, but also because they can reduce carbon dioxide emission caused by Ordinary Portland Cement (OPC) by 80% to 90% in building construction. In this paper, we aim to produce an eco-friendly one-part geopolymer cement with low carbon dioxide emission as an alternative for traditional cements, as well as to conserve the natural resources. The current work focuses on the utilization of industrial wastes rather than natural raw materials with the just-add-water technique for pre-prepared one-part geopolymer cement, which can be applied in various building industries. In the current paper, different types of activators with various ratios and varying firing temperatures from 500 up to 1000°C are studied. The analysis showed that firing of nix at 800°C using 10 and 20% potassium carbonate results in better mechanical strength reaching 550 and 650 Kg/cm^2 after 28 days of hardening.

Funding: Housing and Building National Research Center

Citation: Khater, H.M., El Nagar, A.M., Ezzat, M. Processing, characterization and hardening mechanism of one-part geopolymer cement. Magazine of Civil Engineering. 2022.116(8). Article no. 11611. DOI: 10.34910/MCE.116.11

1. Introduction

The ecological consequences of human activities have come to worldwide attention and are causing environmental concerns all over the globe. In the early and mid-1980s, the concept of sustainable development began spreading [1], while scientists have been striving to make sustainable industrial processes more popular. Industrial ecology is the most efficient way to achieve sustainability [2] by using, in particular, industry-generated by-products. The construction industry contributes to about one-third of the energy-related global CO_2 emissions, which makes it a significant sector often targeted as part of the mitigation strategies to reduce carbon footprint [3]. Since Portland cement is the most common binder used for building materials, its production share amounts to 5–8% of global anthropogenic emissions [4].

With the demand for local cement on the rise, its estimated production may continue to increase in the upcoming years [5]. Clinker production leads to an increase in carbon dioxide emissions through calcination process and fuel combustion. Many studies were conducted to decrease clinker consumption by blending in pozzolanic and cementitious materials, by using an alternative agricultural waste fuel as well. Reduction of CO_2, particularly in this industry, remains a challenge; therefore, many approaches have been proposed to reduce the cement consumption. The use of alternating binders of aluminosilicate minerals can be considered another possible way to reduce the environmental impact of cement [6], which becomes

reactive on activation of suitable materials using alkaline solutions. Through poly-condensation, they turn into a hardened 3D molecule network called geopolymer.

Geopolymer, also referred to as an alkali-activated material, is used as a binder system similar to Portland cement that hardens at room temperature [7]. In addition to that, they have lower carbon footprint compared with Portland cement, exhibit good mechanical properties such as high early strength, excellent resistance to acid, and exceptional resistance to immersion [8]. Curing at an elevated temperature also helps to accelerate the early strength development of geopolymers [9]. However, the traditional synthesis known as the two-part geopolymer, which is typically cured at an elevated temperature system, is difficult to implement in field scale applications [10, 11]. Meanwhile, one-part geopolymer-based binder system uses dry solid aluminosilicate precursors and solid alkali, which form a binder just by adding water, similar to the OPC binder system. In terms of the environmental impacts, an average reduction of 24% for one-part geopolymers and 60% for two-part geopolymers in comparison to OPC were reported in [12].

Researches for developing one-part binders based on the chemistry of alkali aluminosilicate have been largely focused on the mechanical properties produced upon hydration. Other properties related to hydration products of those cements, such as chemical and dimensional stability, moisture and weathering resistance, as well as other hydration properties of these cements have not been investigated.

Additional studies are required to understand more and improve the chemical composition of produced cements, as well as the effectiveness and efficiency of converting raw material blends into hydraulic cements. The produced binder needs to be systematically characterized to qualify for the developed hydraulic cements standards used in concrete production. For the creation of new hydraulic cements, ASTM C1157 [13] and ATSM C559 [14] were the primary performance-based standards employed in this development work. ASTM C1157 criteria are mostly based on ASTM C150 [15] (Standard Specification) performance limitations.

Muthukrishnan et al. [16] looked into the development of early age strength due to alkali reactions in order to formulate a suitable 3D printable one-part geopolymer concrete. On the rheological properties of concrete, the effect of activator content, additives such as magnesium aluminosilicate, and retarder (sucrose) dose were explored. The results showed that the formulated one-part geopolymer with magnesium aluminosilicate, activator, and sucrose content of 0.75 wt%, 10 wt%, and 1.5 wt% of the binder, respectively, performed well.

The main purpose of this research is the production of one-part geopolymer cement that can be produced by just-add-water sequence and applied in building industries by incorporation in mortar and concrete instead of Portland cement with a comparison of its effect on the behavior of the produced materials. The produced materials were expected to be of higher qualification that encourages their use in infrastructure buildings and coastal buildings exposed to severe aggressive medium. The sequence of producing one-part alkali activated cement using various factors was characterized using FTIR, XRD, and SEM; in addition, compressive strength was measured.

2. Material and Methods

2.1. Materials

The material used in this investigation was Egyptian local clay collected from El-Sheik Fadl-Minia, Egypt. The geological setting of the sampling area was studied by Abd El-Wahed [17]. It is composed of clay beds measuring about 25.9 m, as shown in Fig. 1. The clay sections mainly contain dark-colored, gypsiferous clay, highly laminated and fissile in parts. On the other hand, there are two ferrigenous red bands in the upper part, glauconitic shale, and glauconitic sand capped by a nummulitic limestone ledge. In addition, Abd El-Wahed reported that based on the change in color and/or lithology, the clay section is differentiated into 11 beds different in their thickness, the smallest being 0.10 m and the largest – 9 m.

Albite, feldspar, blast furnace slag and cement dust were used as materials enriched in alkalis in addition to sodium and potassium carbonate for production of one-part cement. The chemical compositions of all raw materials are given in Table 1, whereas their mineralogical characterization is presented in Fig. 2. The Egyptian local clay material is formed from montomorlnite, kaolinite, gypsum and quartz. However, albite and feldspar used are composed of muscovite, microcline and albite, just like the main components. Blast furnace slag is mostly amorphous, while cement kiln dust is composed mainly of portlandite, anorthite, sylvite and larnite.

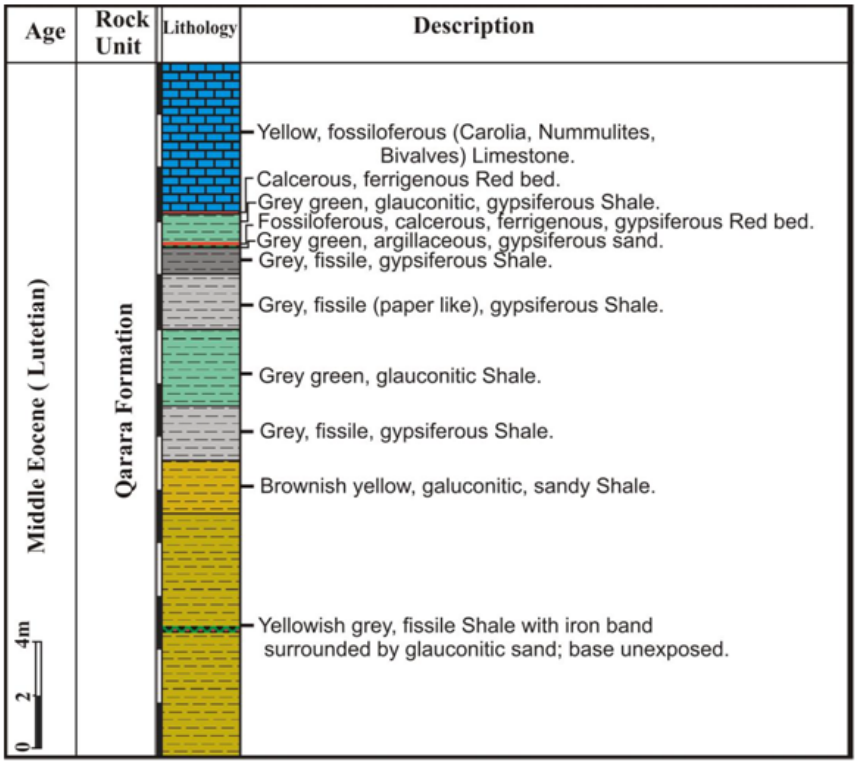

Figure 1. Stratigraphic section of El-Sheikh Fadl sampling area.

Table 1.Chemical composition of starting materials (Mass, %).

Oxide content (%)	SiO_2	Al_2O_3	Fe_2O_3	CaO	MgO	SO_3	K_2O	Na_2O	TiO_2	MnO	P_2O_5	Cl-	L.O.I	BaO	SrO	Total	Notes
BFS	36.67	10.31	0.50	38.82	1.70	2.17	1.03	0.48	0.57	4.04	0.04	0.050	0.12	3.28	0.18	99.96	--
Local Clay	46.80	18.90	8.23	4.02	3.35	1.39	0.70	0.55	1.16	--	0.27	0.66	13.80	--	--	99.82	--
Albite	69.54	14.46	0.13	0.33	0.04	0.03	11.54	3.14	0.01	--	0.03	--	0.66	--	--	99.76	
Feldspar	65.10	17.80	0.42	0.34	0.10	0.03	13.60	2.01	--	--	0.01	0.03	0.49	--	0.02	99.92	--
CkD	4.91	2.12	2.40	49.30	0.61	18.50	5.73	0.32	0.18	0.01	0.08	8.58	6.50	--	--	99.73	Free Lime= 15.50

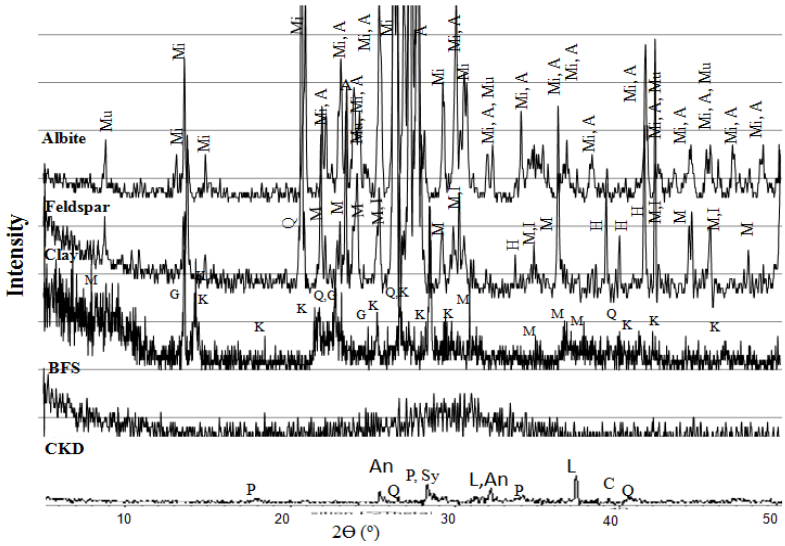

Figure 2. X-Ray diffraction pattern of the starting raw materials. [M: Montomorolnite, I: Illite, G: Gypsum, Q: Quartz, K: Kaolin, Mi: Microcline, Mu:Muscovite, A: Albite, C: Calcite, P:Portlandite, An: Anorthite, L: Larnite, Sy: Sylvite, H: Hematite].

2.2. Geopolymer preparation and curing

One-part geopolymer is prepared by firing the aluminosilicate precursor along with an activator or alkali-rich materials (K_2CO_3, Na_2CO_3, albite, feldspar and CKD) as shown in Table 2 at the requested temperature followed by rapid quenching in order to produce amorphous constituents that can be used for binder production by just-add-water sequence. The fired materials were then sieved in to obtain a fine powder with an average grain size of 90 μm in order to simulate the ordinary cement grain size. The samples were then mixed with tap water, molded and left undisturbed under ambient temperature for 24 hrs in a cube-shaped steel mold, then subjected to curing temperature of 40°C with 100% relative humidity (R.H.) to be able to activate reaction with moderate temperature and simulate the upmost temperature worldwide. At testing time, specimens were removed from their curing conditions, dried well at 80°C for 24 hrs, then tested for their compressive strength. Finally, the resulted crushed specimens were immersed in a stopping solution of methyl alcohol/acetone [18, 19] in order to prevent further hydration, and then preserved in a well tight container until the time of examination.

Table 2. Composition of the geoplymer mixes (Mass, %).

Mix	BFS, %	Clay, %	Na_2CO_3, %	K_2CO_3, %	CKD, %	Albite, %	Feld-spar, %	Wa-ter/ binder	Total M_2O/Al_2O_3	SiO_2/Al_2O_3	Total M_2O/SiO_2
g0	0	100	20	--	--	--	--	0.16	1.11	2.48	0.26
g1	20	80	20	--	--	--	--	0.16	1.22	2.61	0.28
g2	40	60	20	--	--	--	--	0.16	1.36	2.76	0.29
g3	60	40	20	--	--	--	--	0.16	1.53	2.96	0.30
g4	80	20	20	--	--	--	--	0.16	1.76	3.22	0.32
A1	40	60	--	20	--	--	--	0.26	1.09	2.76	0.23
A2	40	60	--	--	20	--	--	0.26	0.21	2.77	0.05
A3	40	60	--	--	--	20	--	0.26	0.29	3.09	0.06
A4	40	60	--	--	--	--	20	0.26	0.29	2.93	0.06
A1-500	40	60	--	20	--	--	--	0.26	1.09	2.76	0.23
A1-600	40	60	--	20	--	--	--	0.26	1.09	2.76	0.23
A1-700	40	60	--	20	--	--	--	0.26	1.09	2.76	0.23
A1-900	40	60	--	20	--	--	--	0.26	1.09	2.76	0.23
A1-1000	40	60	--	20	--	--	--	0.26	1.09	2.76	0.23
A1-T-5	40	60	--	5	--	--	--	0.26	0.36	2.76	0.08
A1-T-10	40	60	--	10	--	--	--	0.26	0.60	2.76	0.13
A1-T-25	40	60	--	25	--	--	--	0.26	1.36	2.76	0.28
A1-T-30	40	60	--	30	--	--	--	0.26	1.58	2.76	0.34

2.3. Methods of investigation

Chemical investigation for starting materials was performed using XRF-Axios (PW4400) WD-XRF Sequential Spectrometer, while mineralogical characterization was performed by using Philips PW 3050/60 Diffractometer with a Cu-Kα source. Mechanical testing was carried out using five tones German Brüf digital compression testing machine with a loading rate of 100 Kg/min. FT-IR was used for elucidation of the amorphous constituents of geopolymer composites using Jasco-6100 with the aid of KBr binder in the range

from 400 to 4000 cm^{-1} [20,21]. Microstructure imaging was done using Scanning Electron Microscopy – SEM Inspect S (FEI Company, Netherland) equipped with an energy dispersive X-ray analyzer (EDX).

3. Results and Discussion

XRD pattern of fired one-part geopolymer cement at 800°C for 2 hrs, having various ratio of blast furnace slag as a partial replacement of local clay mineral and activated by 20% sodium carbonate is presented in Fig. 3. The pattern illustrates an increased intensity of nephline phase [22, 23] as an alkali-rich crystalline phase [(K, Na) $AlSiO_4$].

Moreover, the incorporation of alkali during the thermal pre-activation process resulted in the formation of a new Na-rich phase (a partially disordered per-alkaline aluminosilicate, $[Na_2O]_x$ $[NaAlO_2]_y$ $[NaAlSiO_4]$, represented by phase P in Fig. 2, PDF# 01-076-2385 when x > 0, y = 0; represented by phase Pα, PDF# 00-049-0004, both described below as Na-aluminosilicate for brevity). The last two phases increased up to 40% slag replacement reflecting the disorder of the produced one-part constituent. On increasing slag content to 60%, new phases are formed (sodalites and gehlenite) reflecting increase in crystalline phases with increasing slag ratio [21]. Gehlenite is most likely derived from the chemical interaction between thermally decomposed silicate and alumina derived from the other compounds present in the unreacted clay/slag mix, such as microcline, which are no longer observed in the thermally treated mix.

Larnite was also detected for 60% slag content, reflecting the alteration of the alumina/silica ratio due to participation in the formation of amorphous aluminosilicate constituents. Further increasing of slag ratio up to 80% resulted in the increase of larnite, gehlenite and sodalite phases in addition to the formation of sharp and intense peak of hematite; all the previous phases resulted in diminishing the efficiency of the formed binder.

FTIR spectra of one-part geopolymer cement having various slag ratios and activated by 20% sodium carbonate and fired at 800°C for 2 hrs are shown in Fig. 4. The pattern shows a gradual increase in the main asymmetric band of T-O-Si at about 975 cm^{-1} with minor shifting to lower wave number, where T=Si or Al with increasing slag ratio up to 40%. This is accompanied by diminishing of the shoulder at about 1085 cm^{-1} for un-solubilized silica.

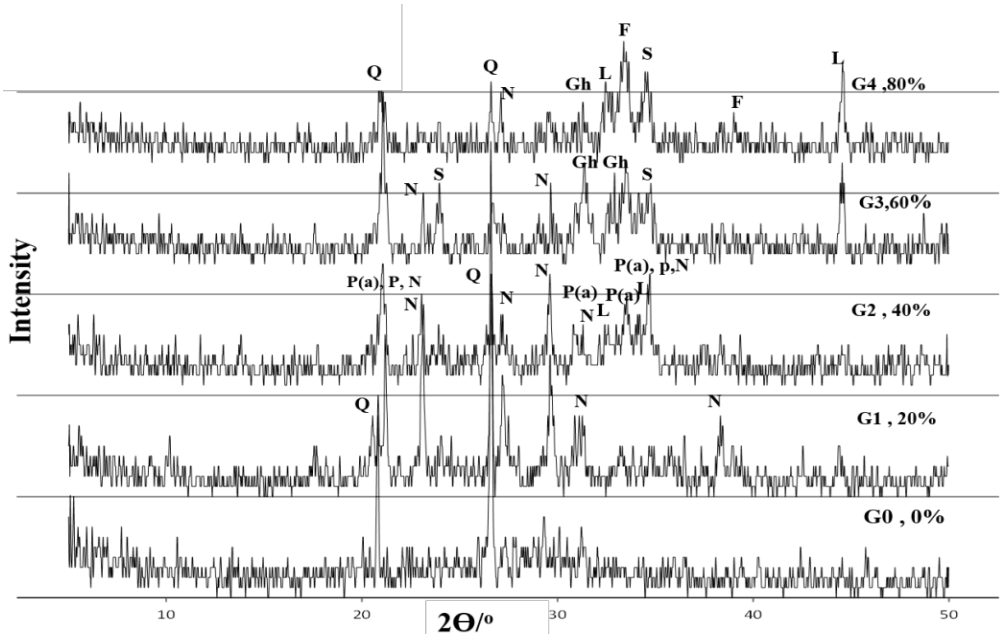

Figure 3. XRD pattern of one-part geopolymer cement having various slag ratios, fired at 800˚C for 2 hrs. [Q: Quartz, N: Nephline, L: Larnite, P: Peralkaline, P(a): Peralkalinealfa, S: Sodalite, Gh: Gehlnite, F: Hematite].

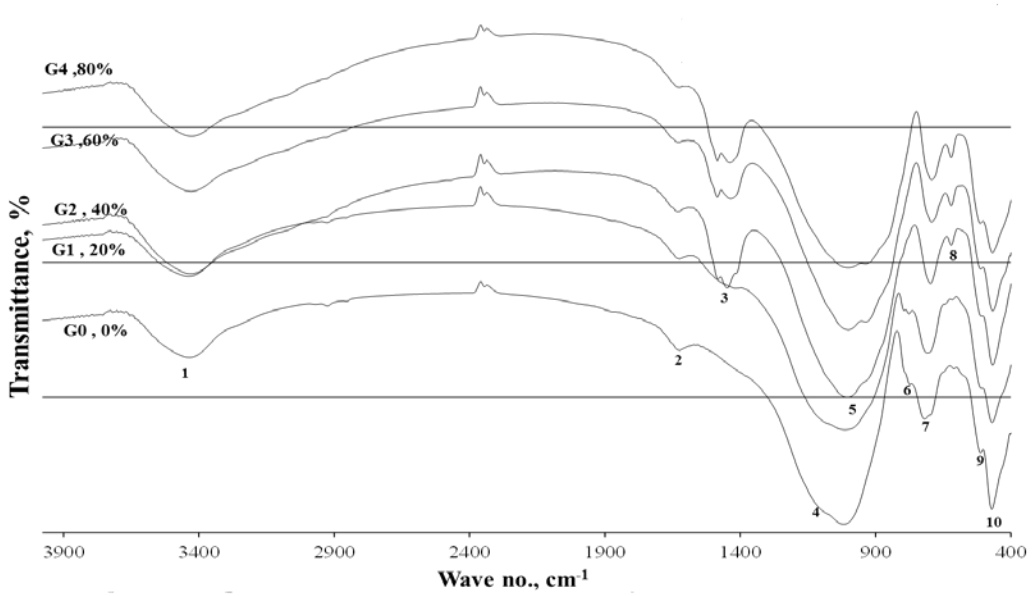

Figure 4. FTIR spectra of one part geopolymer cement having various slag ratios, fired at 800°C for 2 hrs.[1: Stretching vibration of O-H bond, 2: Bending vibrations of (HOH), 3: Stretching vibration of CO2,4: Asymmetric stretching vibration (Si–O–Si), 5: Asymmetric stretching vibration (T–O–Si), 6: Symmetric stretching vibration (Si–O–Al), 7, 8: Symmetric stretching vibration (Si–O–Si), 9,10: Bending vibration (Si–O–Si and O–Si–O)].

The increase of the main asymmetric band on the expense of the un-solubilized silica reflects the increased formation of amorphous N-A-S in accordance with XRD pattern Fig. 3, which depicts the growth of per-alkaline and per-alkaline alfa with slag ratio increasing to 40%. The broad vibration mode appearing between 630 and 690 cm^{-1} is associated with the existence of a range of deformed 4-membered silicate ring structures indicating a disordered state within these solid powders [24, 25]. However, the bands appearing between 750–550 cm^{-1} are related to vibration of silicate ring structures, and a reduction in the wave number within this region associated with a reduced number of bridging oxygen in the corresponding ring structure [25].

On further increasing of slag ratio to 60% and 80%, decrease in intensity of asymmetric band is observed with the splitting of symmetric band at 688 cm^{-1} into two bands at about 613 and 688 cm^{-1} for symmetric stretching of Si-O-Si, as well as its bending vibration. The decreased symmetric stretching vibration of Si-O-Si at about 760 cm^{-1} reflects the increased deformation of the formed binder.

XRD pattern of fired one-part geopolymer cement prepared at 800°C for 2 hrs of 40:60% slag to local Egyptian clay activated by 20% of various activators is presented in Fig. 5. From the pattern, it can be noticed that using of potassium carbonate as an activator results in the formation of an amorphous structure with an increased intensity of Sylvie (KCl), as well as an increased intensity of nephline phase [22, 23] as an alkali-rich crystalline phase [(K, Na) $AlSiO_4$]. Moreover, there is an intense akermanite peak at 2Θ of 31.13°, with the formation of Na-rich phase (a partially disordered per-alkaline aluminosilicate, $[Na_2O]_x$ $[NaAlO_2]_y$ $[NaAlSiO_4]$, represented by phase P in Fig. 2, PDF# 01-076-2385 when x > 0, y = 0; represented by phase Pα, PDF# 00-049-0004, both described below as Na-aluminosilicate for brevity).

Using alkali-rich cement kiln dust results in the formation of crystalline Lucite feldspars, akermanite, as well as larnite phase, which is dicalcium silicate phases susceptible for formation of CSH upon hydration. The increased crystalline phases decrease or diminish disordered aluminosilicate phases. Using sodium carbonate results in the formation of intense peaks of disordered Na-rich phases (per-alkaline and per-alkaline alfa, as well as nephline) as the main phases that favor to be of high reactivity as potassium carbonate. Using feldspar and albite on the other hand, leads to an intense increase in the crystalline phases (albite, muscovite, microcline and mullite), with the formation of small peaks of disordered Na-rich phases. It is clear that the use of the last two activators results in an increase in crystallinity of the formed powder, and thus may negatively affect their hydration performance.

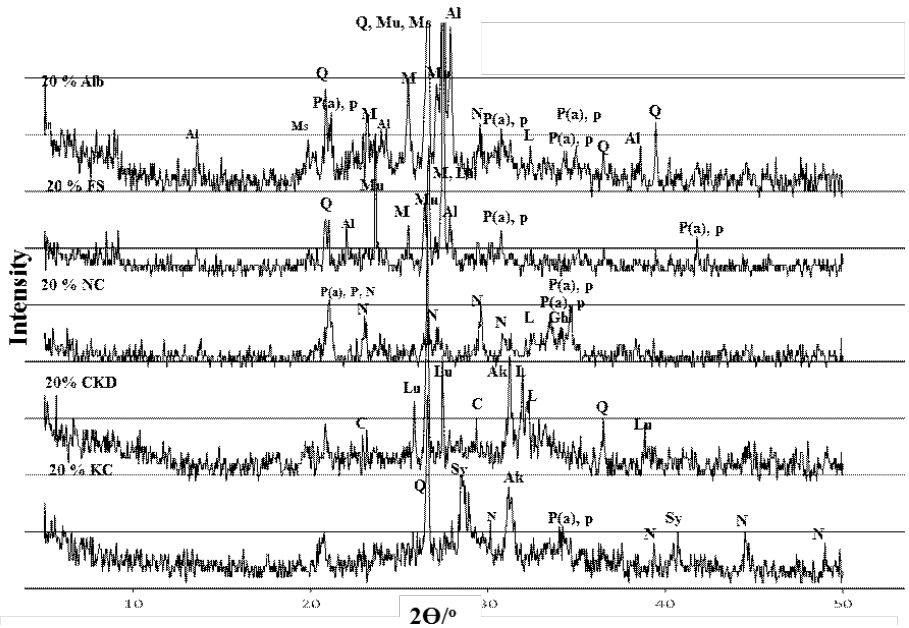

Figure5. XRD pattern of one part geopolymer cement having various types of activators, fired at 800˚C for 2 hrs. [Q:Quartz, Mu: Mullite, M: Microcline, Ms: Muscovite, C: Calcite, Gh: Gehlenite, N: Nepheline, Sy: Sylvite, Lu: Lucite, L: Larnite, Ak: Akermanite, Al: Albite, P: Peralkaline, P(a): Per-alkalinealfa].

FTIR spectra of one-part geopolymer powder having 40:60% slag to local clay activated with various activators and fired at 800°C for 2 hrs are shown in Fig.(6). The pattern illustrates the increased intensity of the main asymmetric band of T-O-Si at about 975 cm^{-1} upon using potassium carbonate activator followed by sodium carbonate one, whereas using cement kiln dust, feldspar and albite results in an increase in intensity of the shoulder at about 1085 cm^{-1} for un-solubilized silica, in the same sequence, which reflects the increase in crystalline phases matching XRD elucidations. The broad vibration mode appearing between 630 and 690 cm^{-1} is associated with the existence of a range of deformed 4-membered silicate ring structures indicating a disordered state within these solid powders activated by K and Na-carbonate, which have intense peaks at this region [24, 25]. The decreased symmetric stretching vibration of Si-O-Al at about 760 cm^{-1} reflects an increase in deformation of the formed binder.

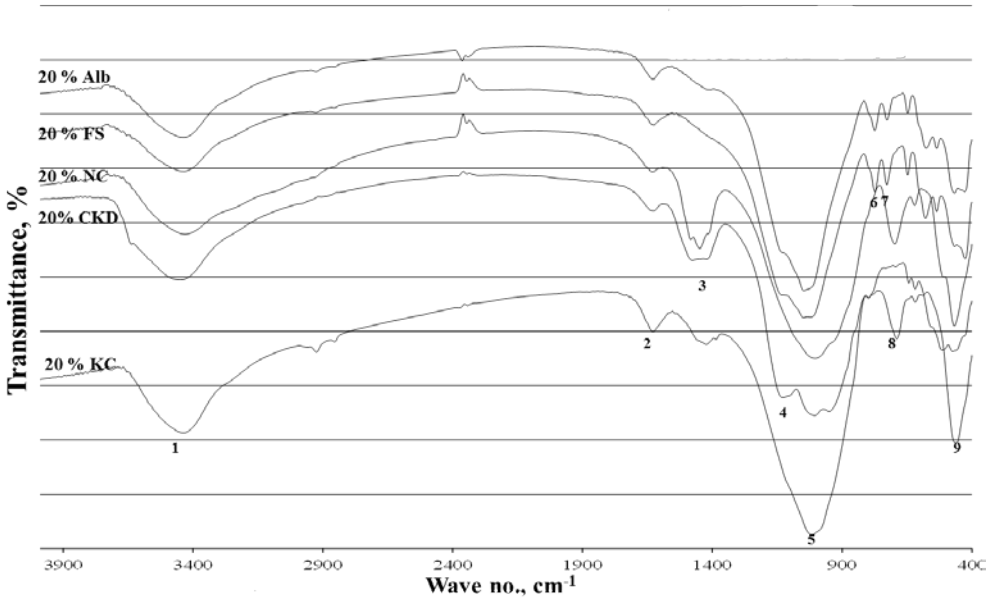

Figure 6. FTIR spectra of one part geopolymer cement having various types of activators, fired at 800˚C for 2 hrs. [1: Stretching vibration of O-H bond, 2: Bending vibrations of (HOH), 3: Stretching vibration of CO_2,4: Asymmetric stretching vibration (Si–O–Si), 5: Asymmetric stretching vibration (T–O–Si), 6,7: Symmetric stretching vibration (Si–O–Al), 8: Symmetric stretching vibration (Si–O–Si), 9: Bending vibration (Si–O–Si and O–Si–O)].

However, elaboration of the transformations was encountered on using various temperatures from 500 to 1000°C for potassium carbonate activated samples; and these variations is noticed using XRD analysis presented in Fig. 7. From the previous pattern, a clear and intense change from amorphous structure which is represented by nephline phase [22, 23] as an alkali-rich crystalline phase [(K, Na) $AlSiO_4$] and Na-rich phase (a partially disordered per-alkaline aluminosilicate phase P and phase Pα with increasing temperature up to 800°C. In addition, there is a gradual transformation from calcium aluminate phases to larnite phases as temperature increased from 500 to 700°C, which both diminishes with the formation of the disordered phases as well as potassium rich sylvite phases at 800°C. Further temperature increase to 1000°C results in the formation of intense peaks for crystalline phases (albite, muscovite, microcline, mullite, gehlinite and hematite), with the formation of small peaks of disordered Na-rich phases. Where, the increase of temperature up 1000°C results in sintering and an increase in crystallinity of the formed powder and so may negatively affect the hydration performance of formed geopolymer.

The FTIR spectra of one-part geopolymer cement activated by potassium carbonate at temperatures ranging from 500 to 100°C for 2 hrs are shown in Fig.(8). The pattern illustrates an increase in intensity of the main asymmetric band of T-O-Si at about 975 cm^{-1} with temperature increase up to 800°C and with a clear decrease in intensity of the shoulder at about 1085 cm^{-1} for un-solubilized silica, in the same sequence, which reflects increase of amorphous structure at the expense of crystalline one coinciding with XRD elucidations. However, further increase in temperature results in sharp decrease in asymmetric band with a shift to left, which implies an increase in crystallinity. A sharp decrease in the carbonate bands as well as O-H bands with temperature up to complete vanishing at 1000°C is noticed.

The broad vibration mode appearing between 630 and 690 cm^{-1} is associated with the existence of a range of deformed 4-membered silicate ring structures indicating a disordered state of these solid powders activated by K and Na-carbonate which have intense peaks at this region increasing up to 800°C, with a decrease in intensity of the symmetric stretching vibration of Si-O-Si at about 760 cm^{-1}, which reflects the increased deformation of the formed binder.

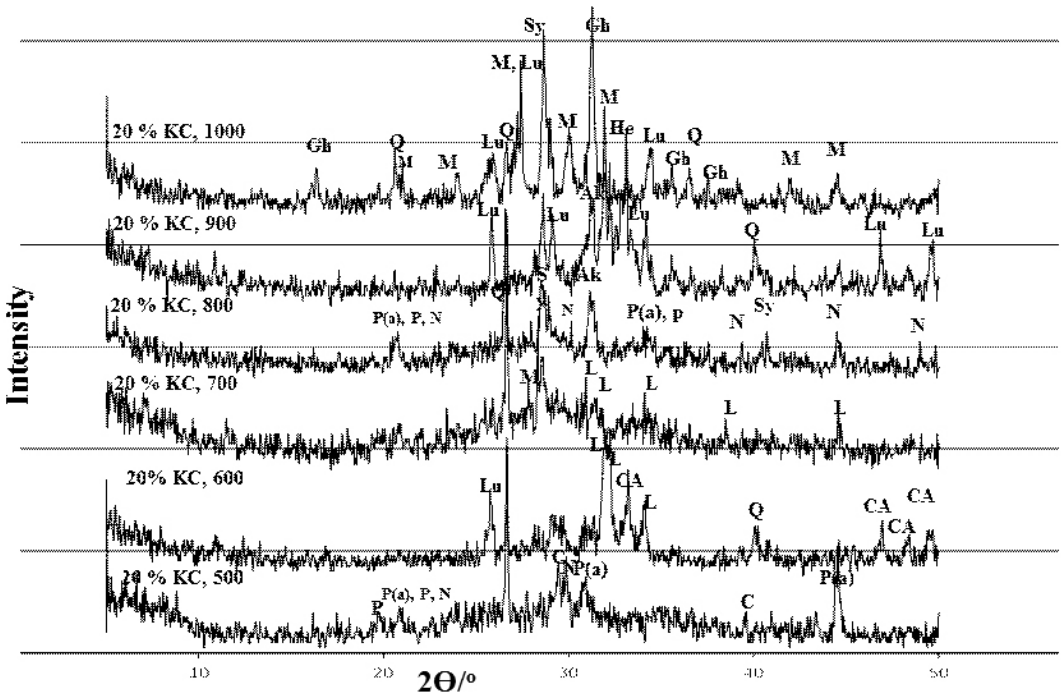

Figure 7. XRD pattern of one part geopolymer cement having various types of activators, fired at 800˚C for 2 hrs. [Q: Quartz, Mu: Mullite, M: Microcline, N: Nepheline, Sy: Sylvite,, Lu: Lucite, L: Larnite, Ak: Akermanite, Gh: Gehlenite, CA: Tricalcium aluminate].

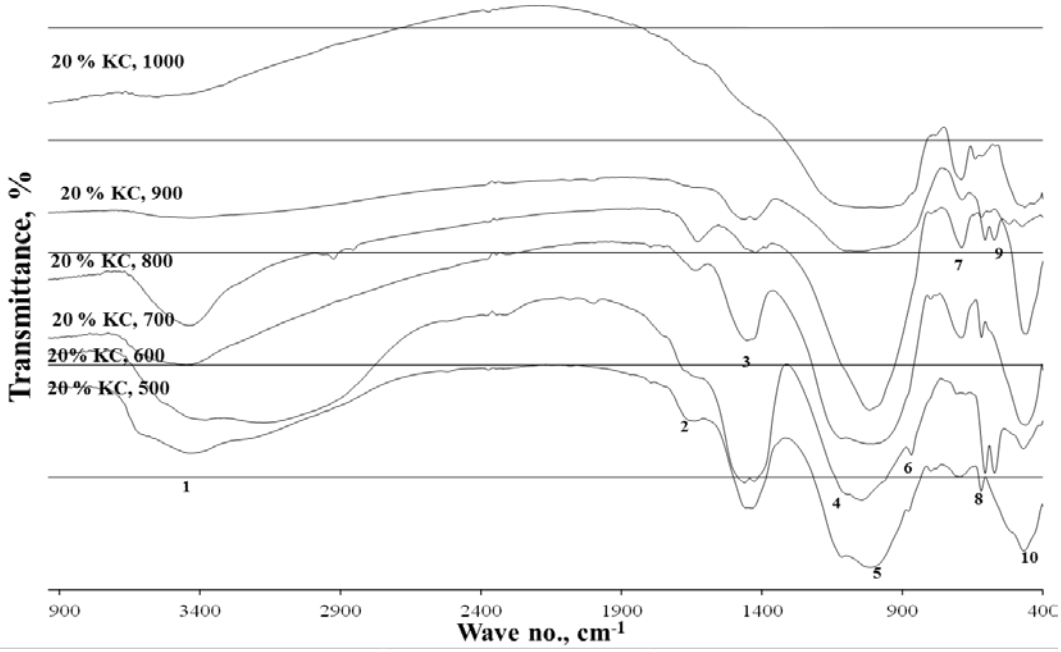

Figure 8. FTIR spectra of one part geopolymer cement having various types of activators, fired at 800˚C for 2 hrs. [1: Stretching vibration of O-H bond, 2: Bending vibrations of (HOH), 3: Stretching vibration of CO_2,4: Asymmetric stretching vibration (Si–O–Si), 5: Asymmetric stretching vibration (T–O–Si), 6: Out of plane bending vibration of CO_2 , 7,8,9: Symmetric stretching vibration (Si–O–Si), 10: Bending vibration (Si–O–Si and O–Si–O)].

On the other hand, using various ratios of potassium carbonate activator from 5 to 30% (Fig. 9) results in a gradual increase in intensity of the main asymmetric band of T-O-Si at about 975 cm^{-1} up to 20% followed by a decrease with further increase in potassium carbonate activator. The shoulder of un-solubilized silica at about 1085 cm^{-1} decreased up to 20%, then was exposed to a gradual increase in intensity up to 30%. The vibration mode appearing between 630 and 690 cm^{-1} for deformed 4-membered silicate ring structures and disordered state, increased sharply up to 30% within these solid powders activated, with nearly diminishing of the symmetric stretching vibration of Si-O-Al at about 760 cm^{-1}, which in turn reflects an increase in deformation of the formed binder.

The results of compressive strength of 28 days of the four groups of hardened one-part geopolymer cement are shown in Fig. 10. In the previous Figure, the strength for one-part mixes activated by 20% Na_2CO_3 having various slag ratios gradually increase with slag ratio up to 40%, giving about 84 Kg/cm^2, while further increase of slag percent results in a decrease in strength, giving about 72 and 66 Kg/cm^2 for 60 and 80% of slag. The strength behavior of this pattern was confirmed by XRD and FTIR, which reflected the increased amorphous content with slag up to 40%. On the other hand, using various activators in the ratio of 20% (Fig. 10B) results in an extra increase in the compressive strength, 650 g/cm^2, for mixes activated by potassium carbonate, while the rest of the used activators acquired strength values of less than 100 Kg/cm^2. As confirmed by XRD and FTIR pattern, there was a sharp increase in disordered phases with a decrease in the crystalline phases on using the potassium carbonate activator, while the crystalline phases were predominant for other mixes incorporating different types of activators leading to strength decline.

However, on using various temperatures for preparation of one-part cement with 20% potassium carbonate and forming of hardened paste (Fig.10C), the strength pattern confirmed that 800°C was the optimal temperature for formation of high strength pastes giving about 650 Kg/cm^2. On varying the ratio of potassium carbonate activator in the mix from 5 to 30%, there was a gradual strength increase up to 650 Kg/cm^2 on using 20% of activator ratio as depicted from (Fig. 10D), while it was clear that on further increase of activator, strength declined down to 375 and 273 Kg/cm^2 for 25 and 30% of activator, respectively.

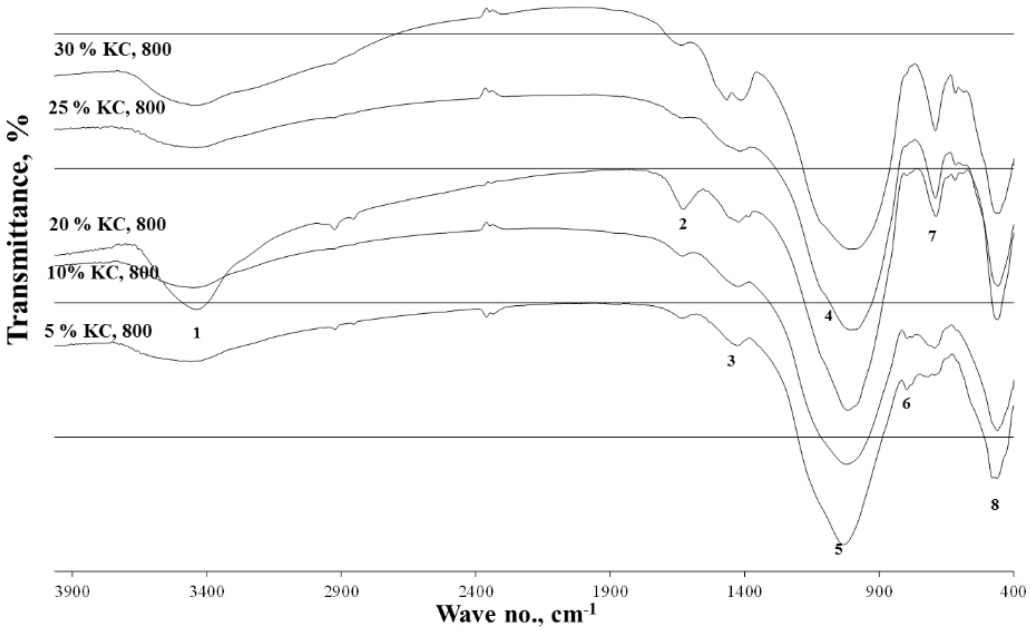

Figure 9. FTIR spectra of one-part geopolymer cement having various ratios of potassium carbonate activator, fired at 800˚C for 2 hrs. [1: Stretching vibration of O-H bond, 2: Bending vibrations of (HOH), 3: Stretching vibration of CO_2, 4: Asymmetric stretching vibration (Si–O–Si), 5: Asymmetric stretching vibration (T–O–Si), 6: Symmetric stretching vibration (Si–O–Al), 7: Symmetric stretching vibration (Si–O–Si), 8: Bending vibration (Si–O–Si and O–Si–O)].

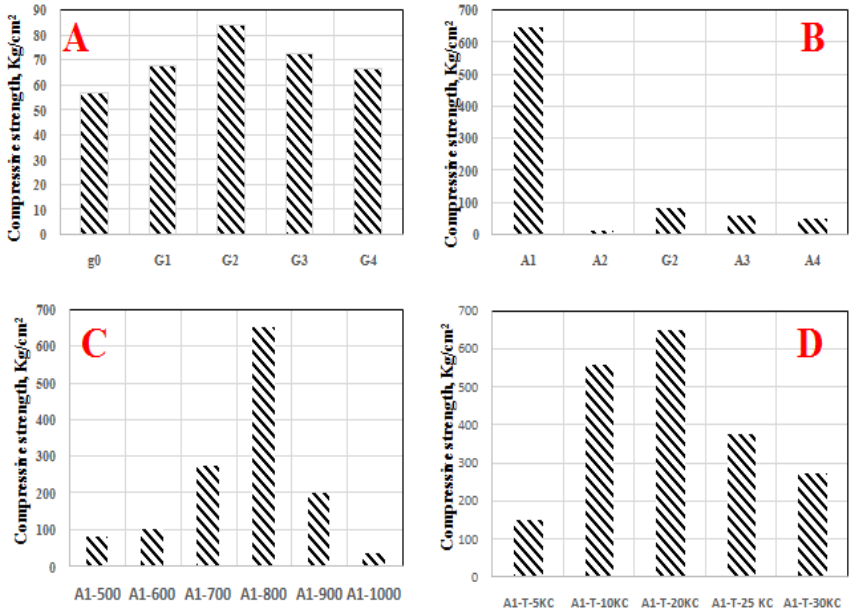

Figure 10. Compressive strength of 28 days of one-part geopolymer cement incorporating; A) various slag ratios, B) various types of activators, C) various firing temperatures for the optimum activators, D) various ratios of optimum activators.

Scanning electron micrographs of 28 days hardened one-part geopolymer pastes prepared by using 20% of different activators fired at 800°C are presented in Fig. 11. It can be observed from the microgpraph (A), that the mix activated by NC, leads to formation of small geopolymer plates with small micropores spreading within the structure. However, the use of KC (B) activator results in the formation of massive geopolymer plates spreading within the matrix. The increased geopolymer structure by using potassium carbonate activator could be attributed to the increased amorphous constituents leading to the formation and growth of the amorphous geopolymer N-A-S-H gel as well as binding gels (C–(A)–S–H resulting in a dense and compact structure [26, 27]. The previous observation is confirmed by the increased compressive

strength of KC sample and by the increased intensity of the asymmetric Si-O-Al in FTIR as well as disordered peralakline phases in XRD. As the use of alkali-rich feldspars (C) results in the formation of heterogeneous structures with little interaction between the formed geopolymer and an increase in porosity within the matrix as well as a spread of carbonates on the matrix, this reflects the low degree of polymerization as a results of low reactivity of the used binder.

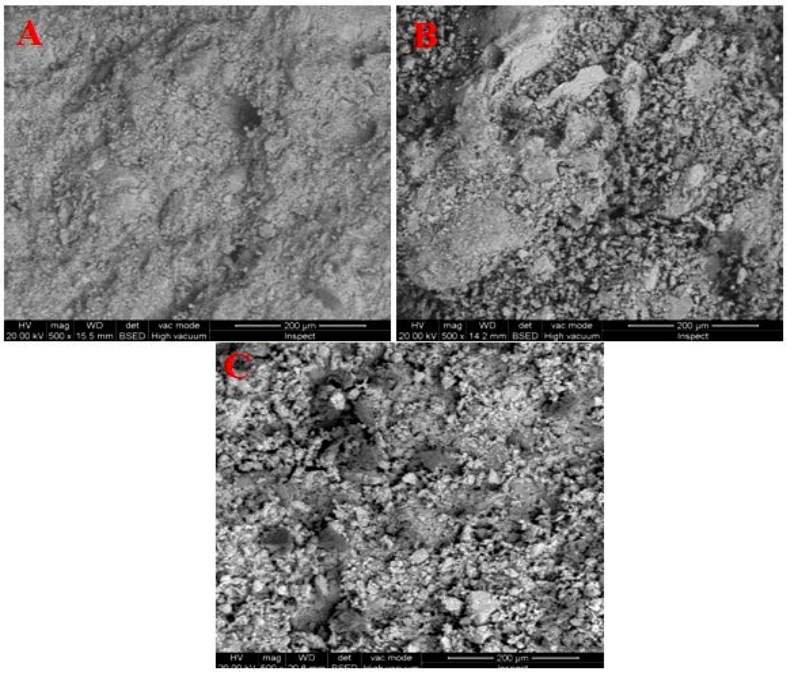

Figure 11. SEM of 28 days of hardened one-part geopolymer cement paste prepared by using different activators; A) 20% NC, B) 20% KC, C) 20% FD.

Scanning electron micrographs of 28 days hardened one-part geopolymer pastes prepared by using 20% K_2CO_3 activator and fired at different temperatures are presented in Fig. 12. The micrographs show the growth of the geopolymer structure with increasing of firing temperature up to 800°C with the formation of massive geopolymer plates (N-A-S-H); while at a lower temperature, small plates are formed in addition to CSH within the matrix. Further increase in temperature to 900°C leads to sintering of the used binder and formation of weakly interacting crystalline structure resulting in formation of low reactivity and affecting the mechanical performance negatively as confirmed by XRD and FTIR.

On the other hand, using various ratios of potassium carbonate activator as presented in Fig. 13 results in the growth of three-dimensional geopolymer network with an increase in activator ratio up to 20%. A higher ratio of activator forms a matrix rich in wide pores, which results in termination of the formed geopolymer chains leading to formation of short chains rather than three dimensional networks [21]. Moreover, the micrograph Fig. 12C illustrates the increase in porosity leading to low cohesion between the reacting particles. Although, the increase in contents of Si and Al in the aqueous phase results in increase in formation of oligomeric precursors by increasing of dissolution rates, extremely high NaOH concentrations inhibit this reaction. As it is seen in Fig. 12, the oligomeric silicate species such as $Si_4O_8(OH)_6^{2-}$ and $Si_4O_8(OH)_4^{4-}$ lose their stability in favor of mononuclear silicate species like $SiO(OH)_3^-$ and $SiO_2(OH)_2^{2-}$ at extremely high alkaline conditions [28]. This means the equilibrium reaction shifted towards monomeric species due to exposure to extremely high alkaline conditions with minimization of the oligomeric silicate species concentration in the aqueous phase and thus led to lower polycondensation rate, which is then measured with the compressive strength of the geopolymeric materials.

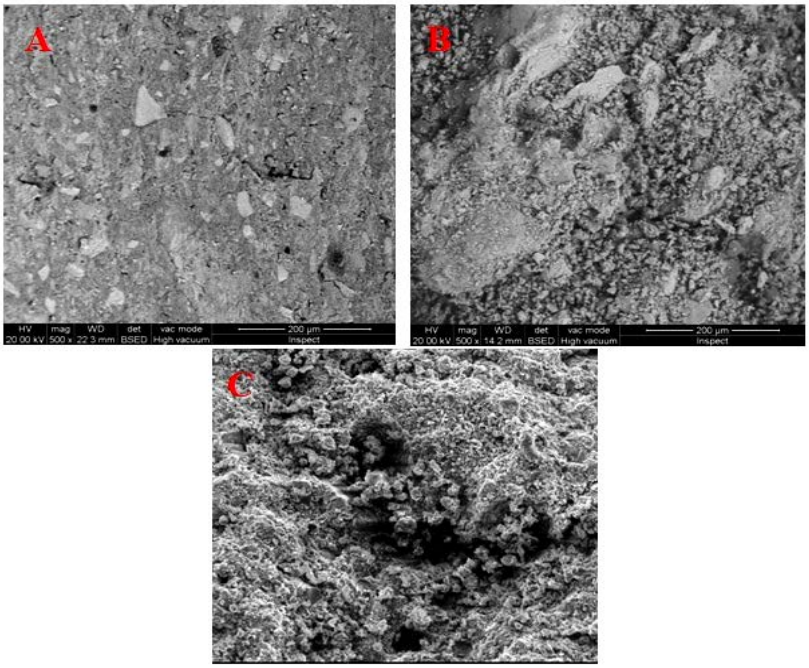

Figure 12.SEM of 28 days of hardened one-part geopolymer cement paste prepared using 20% potassium carbonate, fired at various temperatures; A) 700˚C, B) 800˚C, C) 900˚C.

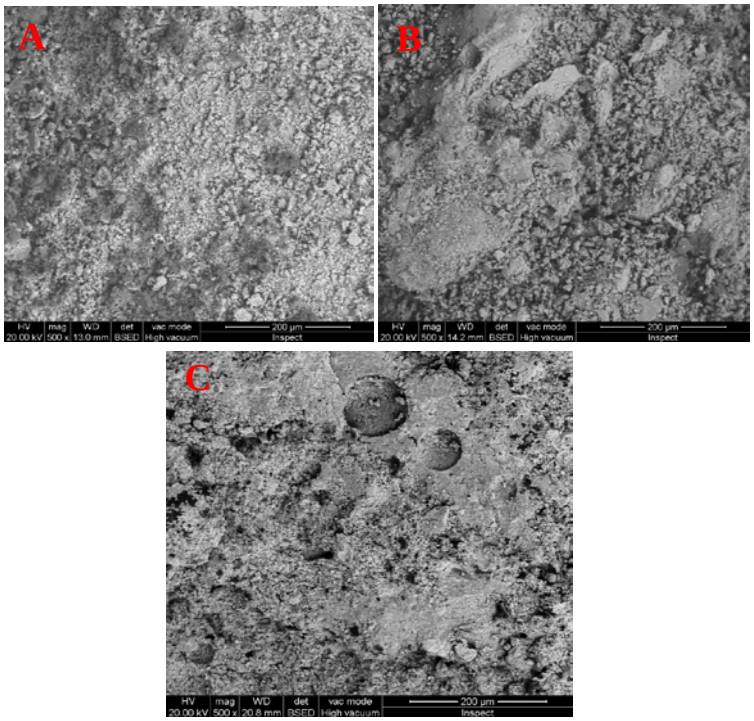

Figure (13): SEM of 28 days of hardened one part geopolymer cement paste formed by various potassium carbonate activator ratios, A) 10 %, B) 20 %, C) 25%.

The elucidations depicted from SEM micrographs can be also confirmed by molar oxide ratios (Table 2). The molar oxide ratios were varied depending on the matrix composition, where the binder formed by activation using potassium carbonate gave SiO2/Al2O3 = 2.48, total alkalis/Al2O3 = 1.11, total alkalis/SiO2 = 0.26. Since the other mixes have high alkalis/Al2O3 more than 1.1 up to 1.76, this increase leads to the consumption of the geopolymer resulting in the formation of short geopolymer chains as confirmed by previously discussed mechanical properties. At the same time, matrix activated by cement kiln dust as well as albite has low alkalis/Al2O3 lower than 0.30. This also coincides with previous data and as stated by [29] for Si/Al ≥ 1.65, the specimens showed a homogenous microstructure as shown in the previous SEM figures, where there is an increased compaction as revealed from interaction between geopolymer constituents, leading to an extra enhancement in matrix performance, which is positively reflected on their mechanical properties as in K2CO3 mix; on the other hand, the use of other activators

leads to formation of crystalline matrix with low mechanical strength. It was suggested that the optimum range of oxide molar ratios [30–32] 0.2<M2O/SiO2<0.48, 3.3<SiO2/Al2O3<4.5, M2O/Al2O3, is 0.8 to 1.6 resulting in three-dimensional networks with a more branched structure, thus forming a homogeneous and compact structure.

4. Conclusions

The main concluded remarks are listed below:

1. Partial replacement of Egyptian local clay by water-cooled slag up to 40% by using sodium carbonate activator and firing at 800°C for 2hrs results in formation of an amorphous powder.

2. Using potassium carbonate activator in the mix results in the formation of predominant disordered aluminosilicate phases.

3. Varying the activation temperature for 20% potassium carbonate samples results in an increased disordered structure up to 800°C, while varying the ratio of K_2CO_3 from 5 to 30% results also in the formation of amorphous phases up to 20%.

4. FTIR and XRD confirm the above-mentioned elucidations.

5. The highest compressive strength of hardened samples for binder activated by 20% K_2CO_3 at 800°C was about 650 Kg/cm^2 after 28 days, and was about 375 Kg/cm^2 and 273 Kg/cm^2 for binder activated by 25% and 30% potassium activator respectively. The performance of the hardened samples is confirmed by SEM micrographs represent a homogenous microstructure for the sample activated by 20% K_2CO_3.

6. The overall results can suggest a low cost simple tool for preparation of one-part geopolymer binder, which can be easily prepared without deleterious effects from activators upon mixing.

References

1. Robinson, J. Squaring the Circle. Some Thoughts on The Idea of Sustainable Development. Ecol. Econom. 2004. 48(4). Pp. 369–384.
2. Blissett, R.S., Rowson, N.A. A Review of the multi-Component utilization of coal fly ssh. Fuel. 2012. 44. Pp. 1–23.
3. Towards a Zero-Emission, Efficient, and Resilient Buildings and Construction Sector: Global Status reports, 2017.[Online].URL: www.worldgbc.org/sites/default/files/UNEP%20188_GABC_en%20%28web%29.pdf (accessed on 15 May 2018).
4. Worrell, E., Price, L., Martin, N., Hendriks, C., Ozawa, M.L.mCarbon Dioxide Emissions from the Global Cement Industry. Annu. Rev. Energ. Environ. 2001. 26. Pp. 303–329.
5. Cement Manufacturers Association of the Philippines Inc (CeMAP). Annual cement Industry Report. Technical Report,+Pasig City, Philippines, 2015.
6. Zhang, Z., Zhu, Y., Yang, T., Li, L., Zhu, H., Wang, H. Conversion of local industrial wastes into greener cement through geopolymer technology: A case study of high-magnesium nickel slag. J. Clean. Prod. 2017. 141. Pp. 463–471.
7. Xie, J., Kayali, O. Effect of initial water content and curing moisture conditions on the development of fly ash-based geopolymers in heat and ambient temperature. Constr. Build. Mater. 2014. 67 (Pt A). Pp. 20–28.
8. Djobo, J.N.Y., Elimbi, A., Tchakouté, H. K., Kumar, S. Mechanical properties and durability of volcanic ash based geopolymer mortars. Constr. Build. Mater. 2016. 124. Pp. 606–614.
9. Peng, M.X., Wang, Z.H., Xiao, Q.G.; Song, F., Xie, W., Yu, L.C., Huang, H.W., Yi, S.J. Effects of alkali on one-part alkali-activated cement synthesized by calcining bentonite with dolomite and Na2CO3. Appl. Clay Sci. 2017. 139. Pp. 64–71.
10. Provis, J.L. Activating solution chemistry for geopolymers. Geopolymers: Structures, Processing, Properties, and Industrial Applications. Woodhead Publishing. Cambridge, UK. 2009. Pp. 50–71.
11. Nematollahi, B.,Sanjayan, J., Shaikh, F.U.A. Synthesis of heat and ambient cured one-part geopolymer mixes with different grades of sodium silicate. Ceram. Int. 2015. 41. Pp. 5696–5704.
12. Luukkonen, T., Abdollahnejad, Z., Yliniemi, J., Kinnunen, P., Illikainen, M. One-part alkali-activated materials: A review. Cem. Concr. Res. 2018. 103. Pp. 21–34.
13. Malenab, R.A.J., Ngo, J.P.S., Promentilla, M.A.B. Chemical Treatment of Waste Abaca for Natural Fiber-Reinforced Geopolymer Composite. Materials. 2017. 10. Pp. 579–589.
14. ASTM C1157. Standard Performance Specification for Hydraulic Cement, ASTM International.West Conshohocken PA, USA, 2011.
15. ASTM C595, Standard Specification for Blended Hydraulic Cements. ASTM International. 15 - West Conshohocken, PA, USA, 2005.
16. ASTM C150, Standard Specification for Portland Cement. ASTM International.West Conshohocken, PA, USA, 2019.
17. Muthukrishnan, S., Ramakrishnan, S., Sanjayan, J. Effect of alkali reactions on the rheology of one-part 3D printable geopolymer concrete. Cement and Concrete Composites. 2021. 116. 10389.
18. Abd El-Wahed, G. Sedimentology and Assessment of the Middle Eocene El Minya Clay Deposits for Ceramic Industries on the Light of their Chemical, Mineral and Microstructure Characteristics. M.Sc. Department of Geology, Mansoura University. 2013.
19. Saikia, N., Usami, A., Kato, S., Kojima, T. Hydration behavior of ecocement in presence of metakaolin. Resource Progressing Journal. 2004. 51 (1). Pp.35–41.
20. Khater, H.M., Influence of metakaolin on resistivity of cement mortar to magnesium chloride solution. Ceramics – Silikáty J. 2010. 54 (4). Pp. 325–333.

21. Vargas, A.S., Denise, C.C. Dal Molin, Ângela, B. Masuero, Antônio.C.F. ; Joao Castro-Gomes; Ruby M. Strength development of alkali-activated fly ash produced with combined NaOH and Ca(OH)2 activators. Cement and concrete composites. 2014. 53. Pp. 341–349.
22. Panias, D., Giannopoulou, I.P., Perraki, T. Effect of synthesis parameters on the mechanical properties of fly ash-based geopolymers. Colloids and Surfaces A: Physicochem. Eng. Aspects. 2007. 301. Pp. 246–254.
23. Buhl, J. C. Synthesis and Characterization of the Basic and Non-Basic Members of the Cancrinite-NatrodavyneFamily.Thermochim. Acta. 1991. 178. Pp. 19–31.
24. Lambert, P., Page, C.L., Short, N.R. Pore Solution Chemistry of the Hydrated System Tricalcium Silicate/Sodium Chloride/Water. Cem. Concr. Res. 1985. 15(4). Pp. 675–680.
25. Ke, X., Bernal, S.A.; Ye, N., Provis, J.L., Yang, J. One-Part Geopolymers Based on Thermally Treated Red Mud/NaOH Blends. J. Am. Ceram. Soc. 2015. 98(1). Pp. 5–11.
26. Sitarz, M., Handke, M., Mozgawa, W. Identification of Silicooxygen Rings in SiO2 Based on IR Spectra. Spectrochim. Acta A. 2000. 56(9). Pp.1819–1823.
27. Khater, H.M. Influence of electric arc furnace slag on characterisation of the produced geopolymer composites. építôanyag J. Silicate Based Compos. Mater. 2015. 67(3). Pp. 82–88.
28. Khater, H.M, El Nagar, A.M. Sustainable production of eco-friendly MWCNT-geopolymer composites with superior sulfate resistance. Advanced composites and hybrid materials,. Springer. 2020. 3. Pp. 375–389.
29. Baes, C. F., Mesmer, R. E. The Hydrolysis of Cations. John Willey & Sons. New York, 1976.
30. Duxson, P., Provis, J. L., Lukey, G. C., Mallicoat, S. W., Kriven, W. M., van Deventer, J. S. J Understanding the relationship between geopolymer composition, microstructure and mechanical properties. Colloids and Surfaces. Colloids and Surfaces A, Physicochemical and Engineering Aspects. 2005. 269 (1-3). Pp. 47–58.
31. Davidovits, J. Mineral Polymers and Methods of Making Them. US Patent 4,349,386, 1982.
32. Davitovits, J., Davitovits, M., Davitovits, N. Process for obtaining a geopolymericalumino-silicate and products thus obtained. US Patent 5,342,595, 1994.
33. Davidovits, J. Chemistry of geopolymeric systems terminology. Proceeding of Second International Conference Geopolymer. 1999. Pp. 9–40.

Information about authors:

Hesham Moustafa Khater, *PhD*
ORCID: https://orcid.org/0000-0002-9832-5895
E-mail: hkhater4@gmail.com

Abdeen El Nagar, *PhD*
ORCID: https://orcid.org/0000-0002-8272-4349
E-mail: abdeenelnagar@yahoo.com

Mohamed Ezzat, *PhD*
ORCID: https://orcid.org/0000-0003-4186-9135
E-mail: topaz75@gmail.com

Received 22.11.2021. Approved after reviewing 31.05.2022. Accepted 01.06.2022.